Polymer Journal (2016) 48, 941–948

www.nature.com/pj

ORIGINAL ARTICLE

Synthesis of hyperbranched poly(ether nitrile)s as supporting polymers for palladium nanoparticles

Mitsutoshi Jikei, Kasumi Nishigaya and Kazuya Matsumoto

A novel hyperbranched poly(ether nitrile) (HBPEN) and its copolymer were synthesized as supports for palladium nanoparticles (PdNPs). Soluble HBPEN and its copolymer were obtained by self-polycondensation of an AB_2 monomer with or without an AB monomer. The study of the model reaction suggested the formation of HBPEN with a degree of branching (DB) of 0.37. Soluble linear poly(ether nitrile) (LPEN) was also synthesized from 2,2-bis(4-hydroxyphenyl)hexafluoropropane and 2,6-difluorobenzonitrile. The coordination of nitrile groups in the repeating unit with Pd^{2+} was confirmed by infrared measurements. The reduction of the coordinated complexes with $NaBH_4$ resulted in the formation of HBPEN-, HBPEN copolymer- and LPEN-supported PdNPs. Both transmission electron microscopy images and X-ray diffraction patterns suggested that PdNPs supported by HBPEN (3.0 ± 0.8 nm) were the smallest in size among these three polymers. A comparison of the three PdNPs suggested that the branched architecture in HBPEN can help prevent the aggregation of PdNPs generated in the early stages of reduction.
Polymer Journal (2016) **48,** 941–948; doi:10.1038/pj.2016.55; published online 1 June 2016

INTRODUCTION

Transition metal nanoparticles (NPs) with sizes of 1–10 nm have been intensively investigated in many fields because of their unique optical, electronic, magnetic and catalytic properties.[1–5] In general, metal NPs are prepared by reduction of the corresponding metal ions in the presence of stabilizers that inhibit undesired aggregation. Alkane thiols are well-known stabilizers for AuNPs.[6] Poly(*N*-vinyl-2-pyrrolidone) is also known as an effective protecting polymer for Cu, Pt, Pd and Ni NPs.[7–10]

Dendrimers are unique three-dimensional, nanosized molecules that have a consecutively branched architecture. There are several examples of the preparation of metal NPs by encapsulating metal ions in dendrimers.[11,12] Polyamidoamine dendrimers are commercially available and have been intensively investigated as supports for metal NPs. The preparation and catalytic activity of metal and bimetal NPs encapsulated by polyamidoamine dendrimers have been reported in the literature.[13–22] Yamamoto and co-workers[23] reported the controlled complexation of metal ions in phenylazomethine dendrimers and subsequent reduction to form metal NPs with a controlled number of atoms. Both of these dendrimers act as isolated nanocarriers to form metal NPs. Hyperbranched polymers, which can be synthesized by a one-step polymerization procedure, are generally recognized as analogs to dendrimers.[24–27] Although hyperbranched polymers have irregularly branched architectures, in contrast to dendrimers, the unique properties derived from dendritic architectures are often observed in hyperbranched polymers. Therefore, metal ions and NPs can be surrounded by a dendritically branched architecture when hyperbranched polymers are used as supports. Hyperbranched polyglycerol-supported Pd, Au, Ag, Pt, Ru and Cu NPs have been reported by several groups.[28–32] Because alkyl-substituted hyperbranched polyglycerols are amphiphilic molecules, stable unimolecular micelles can be formed to encapsulate metal ions. Hyperbranched aramids, polyamidoamines and polyethyleneimines have been reported as supports for metal NPs.[33–41] The interactions of gold, silver and copper ions with primary, secondary and tertiary amino groups in hyperbranched polymers assist in the formation of nanosized metal particles. It has also been noted that the open structure of hyperbranched polymers facilitates the interactions of the metal ions with the internal functional groups.[38,39]

We have previously reported the synthesis of hyperbranched poly(ether nitrile)s (HBPENs) by self-polycondensation of the AB_2 monomer.[42] One of the unique properties of nitrile groups is their ability to coordinate with metal ions. In this study, we report the synthesis of a novel HBPEN that can coordinate palladium ions at the nitrile groups in the repeating units. Subsequent reduction gives palladium nanoparticle (PdNPs) supported by HBPEN. HBPEN copolymer, as a lower-branched HBPEN, and a soluble linear poly(ether nitrile) (LPEN) were also synthesized. The differences in size and distribution of PdNPs supported by HBPEN, HBPEN copolymer and LPEN have been reported with respect to the effect of the dendritically branched architecture on the formation of PdNPs.

EXPERIMENTAL PROCEDURE

Materials

2-Methoxyhydroquinone and 4-(benzyloxy)phenol (BOP) were purchased from Sigma-Aldrich Japan (Tokyo, Japan) and were used as received. 2,6-Difluorobenzonitrile, 2,2-bis(4-hydroxyphenyl)hexafluoropropane, bis

Department of Applied Chemistry, Akita University, Akita, Japan
Correspondence: Professor M Jikei, Department of Applied Chemistry, Akita University, 1-1, Tegatagakuen-machi, Akita-shi, Akita 010-8502, Japan.
E-mail: mjikei@gipc.akita-u.ac.jp
Received 11 February 2016; revised 24 March 2016; accepted 1 April 2016; published online 1 June 2016

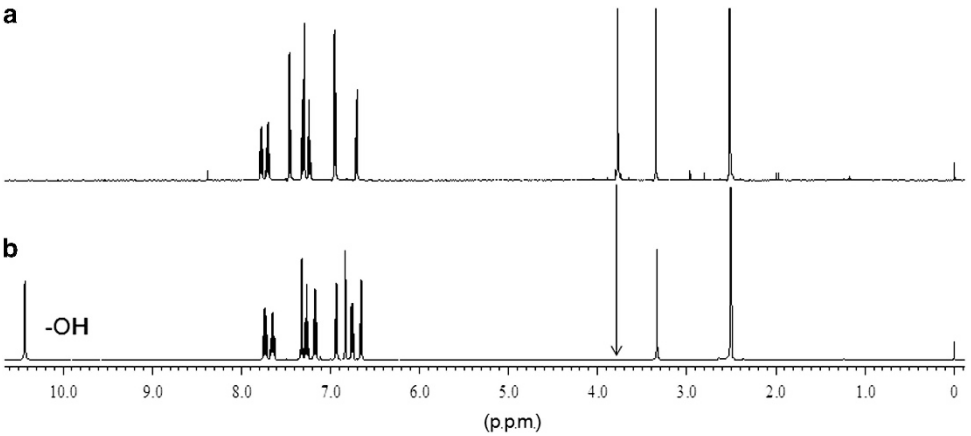

Figure 1 Proton nuclear magnetic resonance (^{1}H NMR) spectra of 2,5-bis(2-cyano-3-fluorophenoxy)anisole (AB_2-OMe) (**a**) and 2,5-bis(2-cyano-3-fluorophenoxy)phenol (AB_2-OH) (**b**).

(benzonitrile)palladium(II) dichloride, cesium fluoride and sodium borohydride were purchased from Tokyo Kasei Kogyo (Tokyo, Japan) and were used as received. Boron tribromide and chloroform were purchased from Nakarai Tesque (Kyoto, Japan) and were used as received. Dichloromethane was purchased from AGC Chemical Company (Tokyo, Japan) and purified by distillation with CaH_2 before use. *N,N*-Dimethylacetamide (DMAc), calcium carbonate and toluene were purchased from Wako Pure Chemical Industries (Osaka, Japan). DMAc was purified by reduced distillation with CaH_2 before use. 3-Methoxyhydroquinone, potassium carbonate, cyclohexane and dimethyl sulfoxide (DMSO) were purchased from Kanto Chemical (Tokyo, Japan) and used as received. Synthesis of a compound used for the model reaction 2,5-bis(2-cyanophenoxy)phenol (AB_0-OH) is described in the Supplementary Information.

Synthesis of AB_2-type monomer

Cesium fluoride (3.108 g, 20.5 mmol) was charged into a two-necked flask equipped with a three-way stopcock. The flask was heat-dried under nitrogen flow, evacuated under vacuum and purged with nitrogen. 2-Methoxyhydroquinone (0.956 g, 6.82 mmol), 2,6-difluorobenzonitrile (2.846 g, 20.5 mmol) and DMAc (15 ml) were added into the flask. The mixture was stirred and heated at 60 °C for 18 h under nitrogen. After cooling to room temperature, the reaction mixture was poured into water. The formed precipitate was collected by filtration and dried under vacuum at room temperature overnight. The yield of AB_2-OMe was 98%. Proton nuclear magnetic resonance (^{1}H NMR) spectrum of 2,5-bis(2-cyano-3-fluorophenoxy) anisole (AB_2-OMe) is provided in Figure 1.

AB_2-OMe (2.540 g, 6.71 mmol) was dissolved in dichloromethane (85 ml) in a two-necked flask equipped with a nitrogen inlet. After cooling with an ice bath for 15 min, boron tribromide (2.6 ml, 26.8 mmol) was added dropwise to the dichloromethane solution. The reaction mixture was stirred with the ice bath for 1 h. After stirring at room temperature for 21 h, the reaction mixture was slowly poured into ice water. The organic layer was extracted with chloroform and concentrated using a rotary evaporator. The crude product was purified by column chromatography in chloroform/ethyl acetate (20/1, v v^{-1}) two times to form a white product. The yield of 2,5-bis(2-cyano-3-fluorophenoxy)phenol (AB_2-OH) was 88%. Anal. calcd for ($C_{20}H_{10}F_2N_2O_3$): C, 65.94; H, 2.77; N, 7.69; found: C, 65.66; H, 3.24; N, 7.58. mp = 190.1 °C. ^{1}H NMR (500 MHz, DMSO-d_6) δ 10.43 (s, 1H), 7.74 (q, 1H, J_{HH} = 8.5, J_{HF} = 6.9 Hz), 7.65 (q, 1H, J_{HH} = 8.6, J_{HF} = 6.9 Hz), 7.33 (d, 1H, J = 8.7 Hz), 7.26 (t, 1H, J = 8.7 Hz), 7.17 (t, 1H, J = 8.7 Hz), 6.94 (d, 1H, J = 8.6 Hz), 6.84 (d, 1H, J = 2.9 Hz), 6.76 (dd, 1H, J = 8.8, 2.9 Hz), 6.66 (d, 1H, J = 8.6 Hz); carbon-13 NMR (^{13}C NMR) (125 MHz, DMSO-d_6) δ 163.1 (d, J_{CF} = 255.5 Hz), 163.0 (d, J_{CF} = 255.4 Hz), 160.8 (d, J_{CF} = 4.1 Hz), 159.9 (d, J_{CF} = 3.6 Hz), 152.4, 150.5, 138.0, 136.5 (d, J_{CF} = 10.2 Hz), 136.2 (d, J_{CF} = 10.8 Hz), 124.0, 113.0 (br), 111.4, 111.2, 110.1, 110.6 (br), 110.3 (d, J_{CF} = 19.2 Hz), 109.2 (d, J_{CF} = 18.6 Hz), 109.1, 92.2 (d, J_{CF} = 18.2 Hz), 90.7 (d, J_{CF} = 18.2 Hz).

Synthesis of AB-type monomer

3-Methoxyphenol (0.620 g, 5.0 mmol) and 2,6-difluorobenzonitrile (0.696 g, 5.0 mmol) were dissolved in DMAc (8 ml) in a two-necked flask equipped with a nitrogen inlet. After addition of potassium carbonate (1.037 g, 7.5 mmol), the flask was heated and stirred at 90 °C for 13 h under nitrogen.[43] After cooling to room temperature, the reaction mixture was poured into water. The formed precipitate was collected by filtration and dried under vacuum at room temperature overnight. The yield of 3-(2-cyano-3-fluorophenoxy)anisole (AB-OMe) was 96%.

AB-OMe was converted to AB-OH in the same manner as described for the synthesis of AB_2-OH from AB_2-OMe. The yield of 3-(2-cyano-3-fluorophenoxy)phenol (AB-OH) was 83%. Anal. calcd for ($C_{13}H_8FNO_2$): C, 68.12; H, 3.52; N, 6.11; found: C, 68.13; H, 4.10; N, 6.13. mp = 127.5 °C.^{1}H NMR (500 MHz, DMSO-d_6) δ 9.87 (s, 1H), 7.70 (q, 1H, J_{HH} = 8.6, J_{HF} = 6.8 Hz), 7.27 (t, 1H, J = 8.2 Hz), 7.24 (t, 1H, J = 8.8 Hz), 6.79 (1H, d, J = 8.6 Hz), 6.71 (dd, 1H, J = 8.2, 2.4 Hz), 6.61 (dd, 1H, J = 8.1, 2.4 Hz), 6.56 (t, 1H, J = 2.1 Hz); ^{13}C NMR (125 MHz, DMSO-d_6) δ 163.1 (d, J_{CF} = 255.5 Hz), 160.0 (d, J_{CF} = 3.8 Hz), 159.1, 155.2, 136.5 (d, J_{CF} = 10.4 Hz), 130.9, 113.0 (d, J_{CF} = 2.4 Hz), 112.7, 111.3, 110.2, 110.0, 106.82, 92.3 (d, J_{CF} = 18.0 Hz).

Self-polycondensation of AB_2-OH to form HBPEN

AB_2-OH (0.75 g, 2.06 mmol), potassium carbonate (0.426 g, 3.09 mmol) calcium carbonate (0.309 g, 3.09 mmol), DMAc (4.5 ml) and toluene (3 ml) were charged into a two-necked flask equipped with a Dean-Stark trap, a nitrogen inlet and a condenser. The reaction mixture was stirred and heated at 150 °C for 1.5 h under nitrogen to remove generated water by azeotropic distillation. The reaction temperature was increased to 160 °C and stirred for 7 h. After diluting with DMAc (10 ml) and cooling to 100 °C, BOP (0.823 g, 4.12 mmol) and potassium carbonate (0.284 g, 2.06 mmol) were added to the reaction mixture. After stirring at 100 °C for 3 h, the reaction mixture was poured into diluted HCl aqueous solution to precipitate the crude product. The crude product was dried under vacuum at room temperature and then purified by precipitation in methanol from chloroform solution. The yield of the product was 80%.

Copolymerization of AB_2-OH and AB-OH to form HBPEN copolymer

AB_2-OH (0.500 g, 1.44 mmol), AB-OH (0.331 g, 1.44 mmol), potassium carbonate (0.597 g, 4.32 mmol), calcium carbonate (0.432 g, 4.32 mmol), DMAc (5 ml) and toluene (3 ml) were charged into a two-necked flask equipped with a Dean-Stark trap, a nitrogen inlet and a condenser. The reaction mixture was stirred and heated at 150 °C for 1.5 h under nitrogen to remove generated water by azeotropic distillation. The reaction temperature was increased to 160 °C and stirred for 5.5 h. After diluting with DMAc (10 ml) and cooling to 100 °C, BOP (0.577 g, 2.88 mmol) and potassium carbonate (0.199 g, 1.44 mmol) was added to the reaction mixture. After stirring at 100 °C

for 3 h, the reaction mixture was poured into diluted HCl aqueous solution to precipitate the crude product. The crude product was dried under vacuum at room temperature and then purified by precipitation in methanol from chloroform solution. The yield of HBPEN copolymer was 72%.

Synthesis of LPEN

2,2-Bis(4-hydroxyphenyl)hexafluoropropane (0.387 g, 1.15 mmol), potassium carbonate (0.477 g, 3.45 mmol), 2,6-difluorobenzonitrile (0.160 g, 1.15 mmol), DMAc (3 ml) and cyclohexane (3 ml) were charged into a two-necked flask equipped with a Dean-Stark trap, a nitrogen inlet and a condenser. The reaction mixture was stirred and heated at 120 °C for 1.5 h under nitrogen to remove generated water by azeotropic distillation. The reaction temperature was increased to 140 °C. After stirring for 18 h, the reaction mixture was poured into diluted HCl aqueous solution. The precipitate was collected by filtration and dried under vacuum at room temperature overnight. The yield of LPEN was 100%.

Condensation of AB_0-OH and AB_2-OMe (model reaction)

AB_2-OMe (0.200 g, 0.53 mmol), AB_0-OH (0.173 g, 0.53 mmol), potassium carbonate (0.110 g, 0.80 mmol) calcium carbonate (0.080 g, 0.80 mmol), DMAc (4.5 ml) and toluene (3 ml) were charged into a two-necked flask equipped with a Dean-Stark trap, a nitrogen inlet and a condenser. The reaction mixture was stirred and heated at 150 °C for 2 h under nitrogen to remove generated water by azeotropic distillation. The reaction temperature was increased to 160 °C and stirred for 1.5 h. After cooling to room temperature, DMAc in the reaction mixture was removed by evaporation. The residual sold was washed with diluted HCl aqueous solution and dried under vacuum for 18 h.

Preparation of HBPEN-Pd^{2+} complex

After dissolving HBPEN (0.180 g) in dichloromethane (6 ml) in a flask, a bis(benzonitrile)palladium(II) dichloride (0.143 g, 0.35 mmol) solution in dichloromethane (6 ml) was added.[44] The mixture was stirred at room temperature for 1 h. The precipitate formed during the reaction was collected by filtration and dried under vacuum overnight. The yield of HBPEN-Pd^{2+} complex was 95%.

Preparation of HBPEN-supported PdNPs

After dissolving the HBPEN-Pd^{2+} complex (20 mg) in DMSO (5 ml) in a flask, sodium borohydride (40.9 mg, 1.08 mmol) in methanol (1 ml) was added to the complex solution. The reaction mixture was stirred at room temperature for 1 h. A small amount (100 μl) of the reaction mixture was pipetted out for transmission electron microscopy (TEM) measurements and the rest of the mixture was poured into water. The precipitate was collected by filtration and dried under vacuum overnight to obtain HBPEN-supported PdNPs.

Measurements

^1H, ^{13}C and ^{19}F NMR (fluorine-19 NMR) spectra were recorded using a JEOL JNM-ECX 500 NMR spectrometer (JEOL, Tokyo, Japan). The inherent viscosity was measured in dimethylformamide at 30 °C at a concentration of 0.5 g dl^{-1}. The gel permeation chromatography measurements with DMAc containing lithium bromide (0.01 mol l^{-1}) as the eluent were carried out using

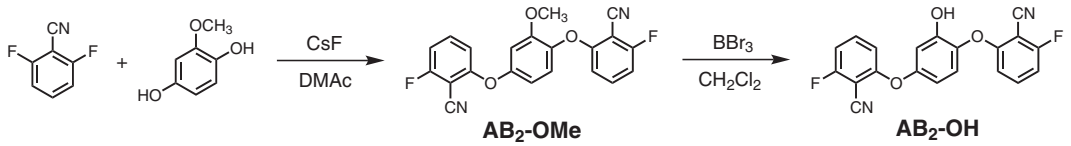

Scheme 1 Synthesis of AB_2-type monomer.

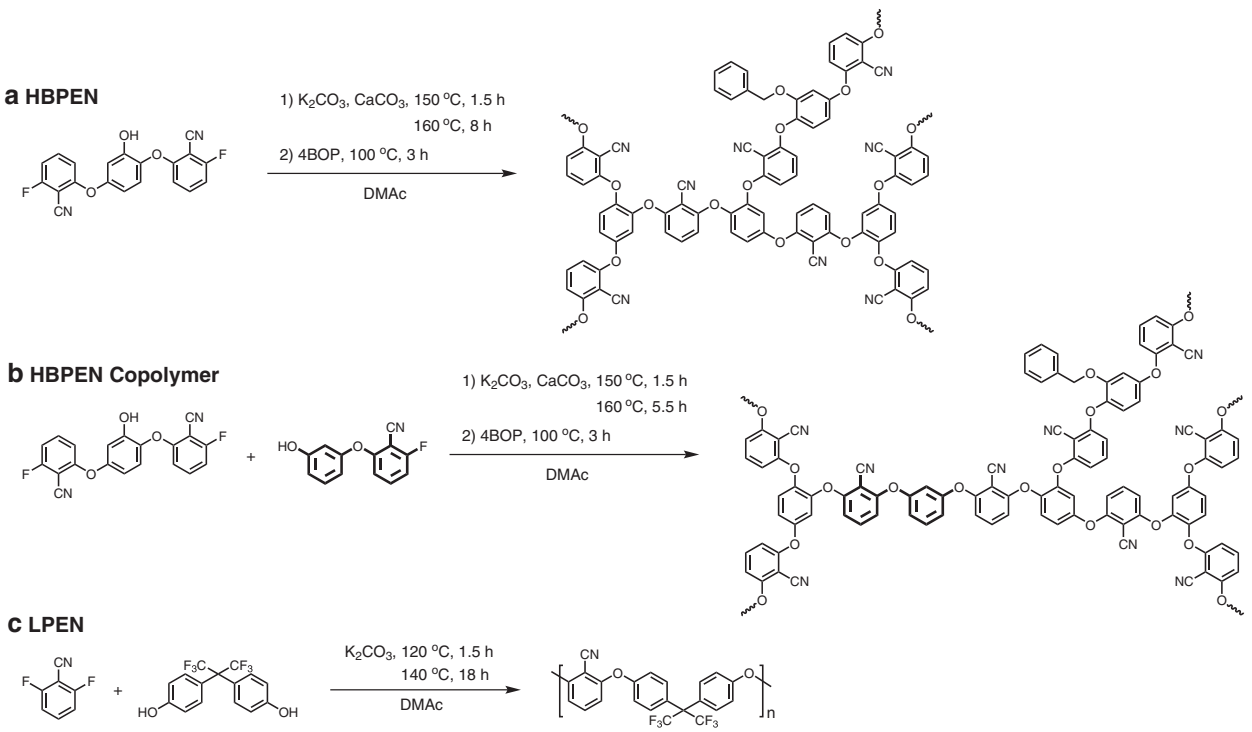

Scheme 2 Synthesis of hyperbranched poly(ether nitrile)s. (**a**) Hyperbranched poly(ether nitrile) (HBPEN); (**b**) HBPEN copolymer; (**c**) linear poly(ether nitrile) (LPEN).

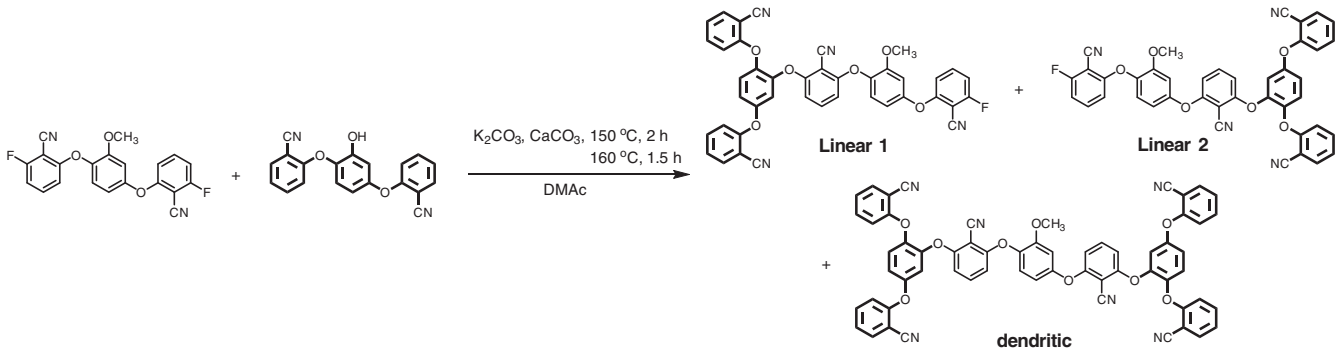

Scheme 3 Condensation of 2,5-bis(2-cyanophenoxy)phenol (AB_0-OH) and AB_2-OMe as a model reaction of self-polycondensation of AB_2-OH.

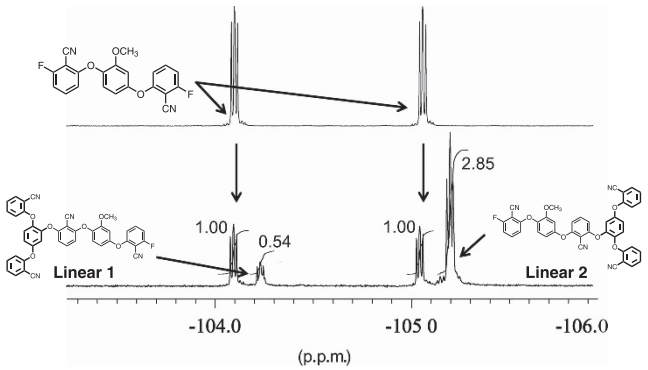

Figure 2 Fluorine-19 NMR (^{19}F NMR) spectra of AB_2-OMe and the resulting compounds.

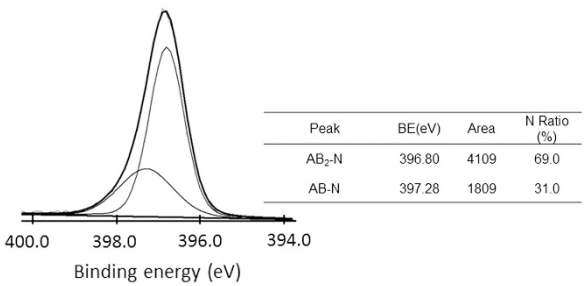

Peak	BE(eV)	Area	N Ratio (%)
AB_2-N	396.80	4109	69.0
AB-N	397.28	1809	31.0

Figure 3 X-ray photoelectron spectroscopy (XPS) spectrum of hyperbranched poly(ether nitrile) copolymer synthesized from AB_2-OH and AB-OH.

a Wyatt DAWN HELEOSII 8 (Wyatt Technology, Santa Barbara, CA, USA), a Wyatt Optilab rEX differential refractometer (Wyatt Technology) and a polystyrene-divinylbenzene column (Tosoh TSK gel GMH_{HR}-M, Tokyo, Japan). The specific refractive index increment (d*n*/d*c*) at 658 nm was measured using a Wyatt Optilab rEX differential refractometer. The d*n*/d*c* values of HBPEN, HBPEN copolymer and the linear polymer in DMAc containing lithium bromide (0.01 mol l^{-1}) were determined to be 0.178, 0.197 and 0.0991 (ml g^{-1}), respectively. Infrared (IR) spectra were recorded on a Thermo Fisher Scientific iS50 FTIR spectrometer (Yokohama, Japan). X-ray photoelectron spectroscopy (XPS) was conducted with a Shimadzu Kratos AXIS-ULTRA spectrometer (Kyoto, Japan). Thermogravimetric measurements were performed on a Hitachi High-Technologies STA7300 (Tokyo, Japan) at a heating rate of 10 °C min^{-1}. TEM measurements were performed using a JEM-1200XII (JEOL, Tokyo, Japan) with an acceleration voltage of 120 kV. The PdNPs solution in DMSO was diluted with chloroform and drop-casted on a carbon grid (NS-C15; Okenshoji, Tokyo, Japan) for TEM measurements. The mean particle size and its distribution were evaluated by measuring 100 particles in the TEM images. Wide-angle X-ray diffraction measurements were conducted using a RIGAKU Ultima IV X-ray diffractometer (Tokyo, Japan).

RESULTS AND DISCUSSION

Synthesis of HBPEN

An AB_2-type monomer containing two nitrile groups was prepared from 2-methoxyhydroquinone and 2,6-difluorobenzonitrile as starting materials (Scheme 1). The selective monosubstitution of 2,6-difluorobenzonitrile proceeded by condensation at 60 °C for 18 h to form AB_2-OMe. The structure of AB_2-OMe was confirmed by ^{1}H NMR spectroscopy, as shown in Figure 1a. Because AB_2-OMe is asymmetric, two sets of peaks were observed for aromatic protons derived from the fluorobenzonitrile unit. For example, two quartet peaks were observed at 7.73 and 7.65 p.p.m., which were attributed to aromatic protons para to nitrile groups. All other peaks were assigned to the proposed structure, and the integration ratio of the peaks supported the formation of AB_2-OMe. Conversion of the methoxy group to a hydroxy group was performed by the reaction of AB_2-OMe with boron tribromide. A white powdery product (AB_2-OH) was obtained after purification by column chromatography. As shown in Figure 1b, the peak attributed to methoxy protons of AB_2-OMe (3.8 p.p.m.) disappeared, and a new peak attributed to the hydroxy proton was observed at 10.4 p.p.m. An H-H COSY (H-H COrrelation SpectroscopY), ^{13}C NMR spectra and the detailed assignment of the peaks are provided in the Supplementary Information. The integration ratios of the peaks also supported the formation of AB_2-OH.

Self-polycondensation of AB_2-OH was performed at 160 °C to form HBPEN, as shown in Scheme 2a. In addition to potassium carbonate, calcium carbonate was added to the reaction mixture to minimize potential ether exchange reactions.[45] The solution viscosity increased during the self-polycondensation at 160 °C. The addition of BOP to convert the terminal groups to 4-(benzyloxy)phenyl ether decreased the solution viscosity of the reaction mixture. HBPEN with benzyloxyphenyl ether terminals was obtained by pouring the mixture into acidic water. The reason for the increase in the solution viscosity before the conversion of terminal groups is unclear. We assume that it is caused by the intermolecular interactions between fluoride–hydrogen or fluoride–fluoride groups. The molecular weight of HBPEN, determined by gel permeation chromatography with a light-scattering detector, was 2.56×10^5 g mol^{-1}. HBPEN is soluble in chloroform, DMAc and DMSO and insoluble in methanol.

The degree of branching (DB) is one of the most important parameters in determining the ratio of dendritic, linear and terminal units in hyperbranched polymers. It was impossible to directly determine the DB of HBPEN because of broadening of the peaks in the NMR spectra. Therefore, DB was indirectly estimated by a model

reaction, shown in Scheme 3. The condensation of AB_0-OH and AB_2-OMe at a molar ratio of 1:1 was performed, and the amount of unreacted fluoro groups in the reaction mixture was quantitatively evaluated by ^{19}F NMR spectroscopy. The disubstitution of fluoro groups in AB_2-OMe reflects the formation of dendritic units, which are not observed in ^{19}F NMR measurements. Instead, the amount of unreacted AB_2-OMe is equal to that of the dendritic units remaining in the reaction mixture. Therefore, the integration ratio of the peaks originating from AB_2-OMe to the newly observed ones originating from linear units allows calculation of DB according to the equation $DB = 2D/(2D+L)$, where D and L represent the number of dendritic and linear units, respectively. As shown in Figure 2, AB_2-OMe showed two triplet peaks at −104.1 and −105.1 p.p.m. New peaks were observed at −104.2 and −105.2 p.p.m., which implied the formation of linear **1** and linear **2** compounds. The DB calculated from the integration ratio was 0.37, which is lower than the statistically expected value of 0.5 for hyperbranched polymers synthesized from AB_2 monomers. Because AB_2-OMe is asymmetric, the reactivity of the B functional groups (fluoro groups) is not equal to nucleophilic substitution reactions. The highly reactive B functional groups preferentially react with the A function, which prefers to form the linear compound rather than the dendritic compound.[46] Therefore, the low DB could have been caused by the asymmetric structure of AB_2-OMe.

Equimolar amounts of AB_2-OH and AB-OH were copolymerized to synthesize HBPEN with a lower DB, as shown in Scheme 2b. Terminal fluoro groups of the copolymer were converted to 4-(benzyloxy) phenyl ether, similar to HBPEN. It was impossible to determine the composition ratio of each unit because of peak broadening in the ^1H NMR spectrum. The composition ratio was evaluated from narrow-scan XPS spectra, as shown in Figure 3. The peaks at 396.80 and 397.28 eV were attributed to N 1 s originating from AB_2-OH and AB-OH, respectively. The area ratio after the curve-fitting of these two peaks was 69:31, which is almost consistent with the expected ratio according to the feed molar ratio of AB_2-OH and AB-OH. The incorporation of the AB-OH unit in the resulting polymer statistically lowers the DB. Thus, an HBPEN copolymer having a low DB was successfully obtained from the copolymerization.

It has been reported that poly(ether nitrile) synthesized from resorcinol and difluorobenzonitrile is insoluble in common organic solvents.[47] To synthesize soluble LPEN, 2,2-bis(4-hydroxyphenyl) hexafluoropropane and 2,6-difluorobenzonitrile were polymerized, as shown in Scheme 2c. The results for the synthesis of poly(ether nitrile) s are summarized in Table 1. The weight-average molecular weight (M_w) of all the polymers suggests the formation of high-molecular-weight polymers. HBPEN showed a high M_w and a low inherent viscosity, typical of hyperbranched polymers.

Table 1 Synthesis of poly(ether nitrile)s

	M_w (g mol^{-1})	dn/dc (ml g^{-1})	η_{inh} (dl g^{-1})
HBPEN	2.56×10^5	0.178	0.18
HBPEN copolymer	7.44×10^4	0.197	0.18
LPEN	4.85×10^4	0.099	0.40

Abbreviations: η_{inh}, inherent viscosity; dn/dc, specific refractive index increment; HBPEN, hyperbranched poly(ether nitrile); LPEN, linear poly(ether nitrile); M_w, weight-average molecular weight.

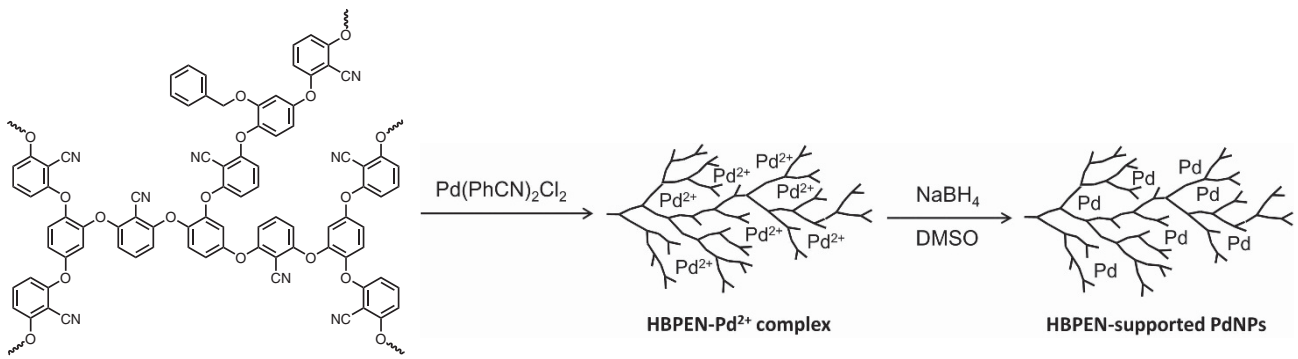

Scheme 4 Preparation of hyperbranched poly(ether nitrile)-Pd^{2+} (HBPEN-Pd^{2+}) complex and HBPEN-supported palladium nanoparticles (PdNPs).

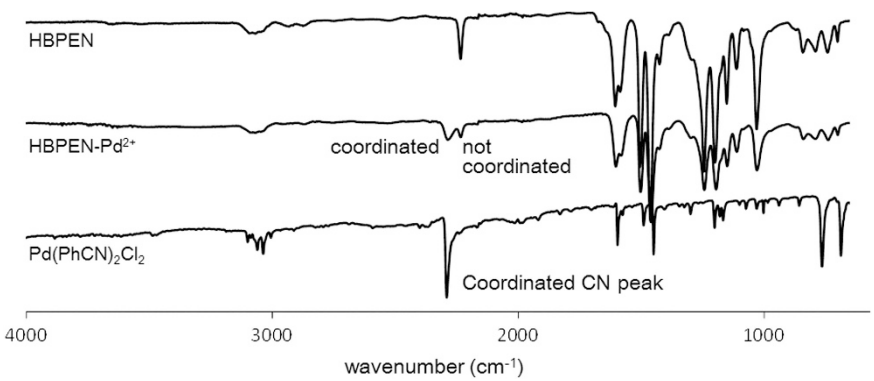

Figure 4 Infrared (IR) spectra of hyperbranched poly(ether nitrile) (HBPEN), HBPEN-Pd^{2+} complex and $Pd(PhCN)_2Cl_2$.

Table 2 Quantitative analysis of polymer-Pd^{2+} complexes by XPS measurement

Complex	*Atomic ratio (N/Pd)*	*Pd^{2+} content (wt%)*
HBPEN-Pd^{2+}	2.85	11.5
HBPEN copolymer-Pd^{2+}	4.05	9.1
LPEN-Pd^{2+}	2.79	7.6

Abbreviations: HBPEN, hyperbranched poly(ether nitrile); LPEN, linear poly(ether nitrile); Pd, palladium; XPS, X-ray photoelectron spectroscopy.

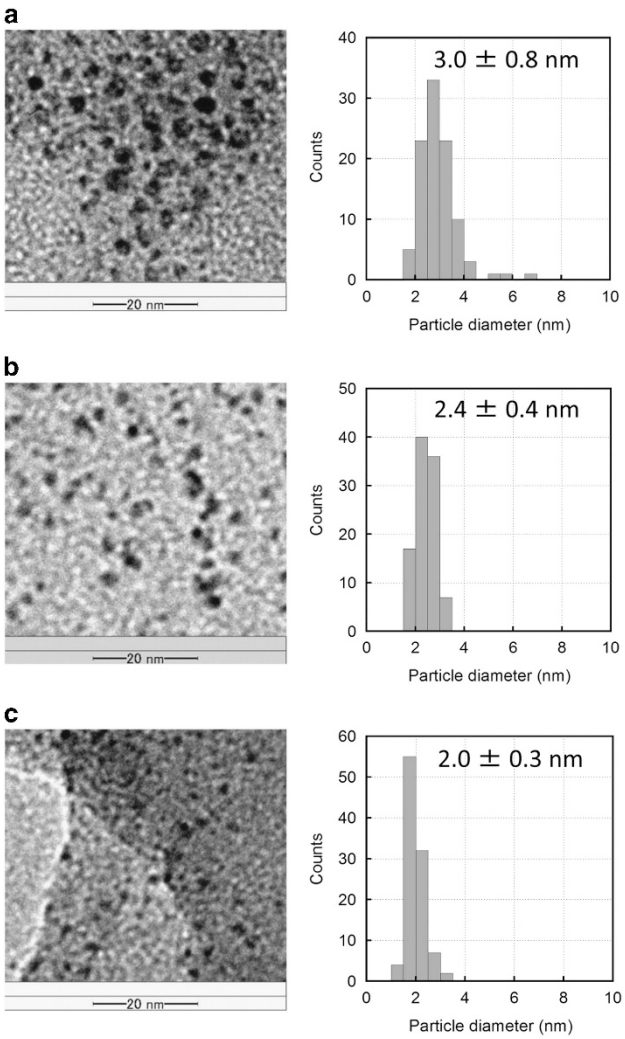

Figure 5 Transmission electron microscopy (TEM) images and histograms of hyperbranched poly(ether nitrile) (HBPEN)-supported palladium nanoparticles (PdNPs) in reaction mixture. (**a**) No additional HBPEN; (**b**) additional HBPEN (five times by weight) was added to the complex solution; (**c**) additional HBPEN (7.5 times by weight) was added to the complex solution.

Preparation of PdNPs

An HBPEN-Pd^{2+} complex was prepared by a ligand exchange reaction described in the literature,[44] as shown in Scheme 4. The HBPEN-Pd^{2+} complex was precipitated during the ligand exchange reaction. IR spectra of HBPEN, HBPEN-Pd^{2+} complex and $Pd(PhCN)_2Cl_2$ are shown in Figure 4. The CN stretching vibration of HBPEN was observed at 2230 cm^{-1}. A new peak attributed to coordinated

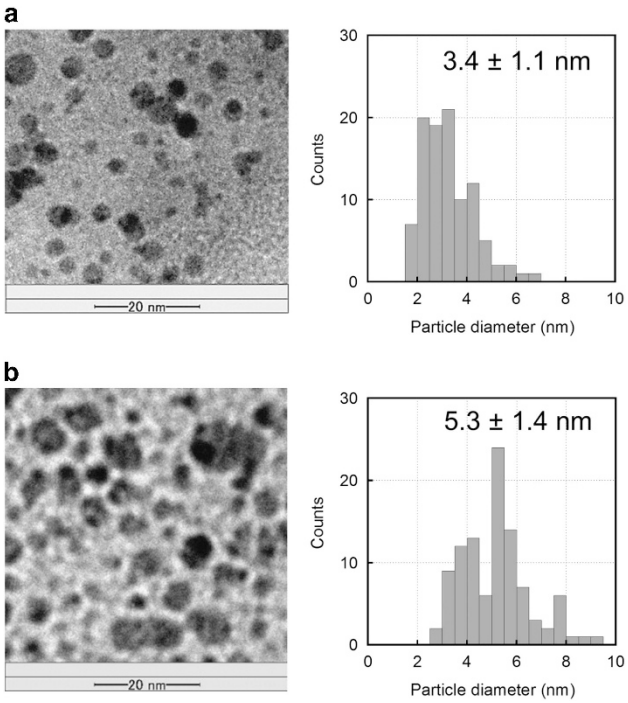

Figure 6 Transmission electron microscopy (TEM) images and histograms of hyperbranched poly(ether nitrile) (HBPEN) copolymer-supported palladium nanoparticles (PdNPs) (**a**) and linear poly(ether nitrile) (LPEN)-supported PdNPs (**b**).

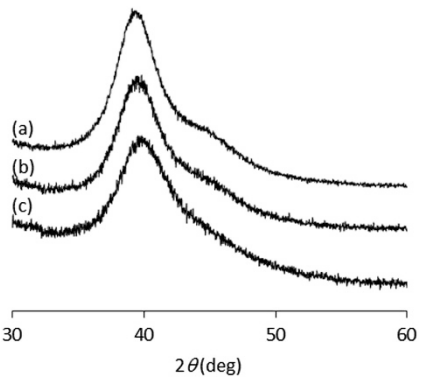

Figure 7 X-ray diffraction (XRD) patterns of polymer-supported palladium nanoparticles (PdNPs). (**a**) Hyperbranched poly(ether nitrile) (HBPEN)-supported PdNPs; (**b**) HBPEN copolymer-supported PdNPs; (**c**) linear poly(ether nitrile) (LPEN)-supported PdNPs.

Table 3 XRD data of polymer-supported PdNPs

PdNPs	*2θ (deg)*	d *(Å)*
HBPEN-supported	39.554	2.2765
HBPEN copolymer-supported	39.561	2.2761
LPEN-supported	39.795	2.2633

Abbreviations: HBPEN, hyperbranched poly(ether nitrile); LPEN, linear poly(ether nitrile); PdNP, palladium nanoparticle; XRD, X-ray diffraction.

CN groups was observed at 2290 cm^{-1} in the spectrum of the HBPEN-Pd^{2+} complex; a peak attributed to non-coordinated CN groups was also observed. The peaks attributed to a C–H out-of-plane deformation vibration disappeared in the spectrum of the HBPEN-Pd^{2+}

complex, which implies that the benzonitrile originating from Pd $(PhCN)_2Cl_2$ was not present in the HBPEN-Pd^{2+} complex. The coordination of nitrile groups with Pd^{2+} in HBPEN enables the initial formation of PdNPs in the dendritically branched architecture during the subsequent reduction step. The HBPEN copolymer-Pd^{2+} and LPEN-Pd^{2+} complexes were also prepared in the same manner as the HBPEN-Pd^{2+} complex. IR spectra of the HBPEN copolymer-Pd^{2+} and LPEN-Pd^{2+} complexes indicated the presence of coordinated CN groups in the complexes. XPS measurements were performed to determine the Pd^{2+} content in the complexes (Table 2). The palladium contents were in the range of 7.6–11.5 wt%.

HBPEN-supported PdNPs were prepared by reduction of the Pd^{2+} complexes with $NaBH_4$. TEM images of the PdNPs (Figure 5a) indicated that the mean particle size was 3.0 ± 0.8 nm. The small particle size and narrow-size distribution suggest that the dendritically branched architecture in HBPEN prevents the aggregation of PdNPs generated in the early stage of the reduction. Extra HBPEN added to the HBPEN-Pd^{2+} complex solution before the reduction was effective to reduce the particle size and distribution. When five times the initial amount of HBPEN by weight was added to the complex solution, the mean particle size decreased to ~2.4 nm (Figure 5b). The smallest PdNPs in this study (2.0 ± 0.3 nm) were observed when 7.5 times the initial amount of HBPEN was added (Figure 5c). Because HBPEN has an irregularly branched architecture, in contrast to dendrimers, the coordination sites in the HBPEN-Pd^{2+} complex are distributed from the inside to the periphery of HBPEN. We assume that Pd^{2+} ions located near the periphery can be surrounded by the additional HBPEN to prevent the aggregation of PdNPs.

PdNPs supported by HBPEN copolymer and LPEN were also prepared by the same procedure described for HBPEN-supported PdNPs (Figure 6). The size and distribution of PdNPs supported by the HBPEN copolymer slightly increased to 3.4 ± 1.1 nm. Because the HBPEN copolymer has a lower DB in comparison with its homopolymer (HBPEN), the number of palladium ions surrounded by the dendritic branches could be decreased. Therefore, the probability of forming aggregates of PdNPs increased, which resulted in the slightly larger size and distribution. The particle size and distribution markedly increased when the LPEN-Pd^{2+} complex was reduced to form PdNPs (5.3 ± 1.4 nm). These data suggest that the dendritic branches in the HBPEN architecture effectively prevent the aggregation of PdNPs generated in the early stages of the reduction.

It has been reported that small PdNPs exhibit an unusual lattice expansion, which can be observed by a peak shift in the X-ray diffraction measurements.[9,48,49] Figure 7 and Table 3 show X-ray diffraction data for PdNPs supported by HBPEN, HBPEN copolymer and LPEN. The diffraction angle and interplanar spacing of the {1 1 1} plane of palladium black are reported to be 40.080° and 2.2478Å, respectively.[9] The diffraction angles of PdNPs in this study were all smaller than that of palladium black. The smallest diffraction angle at 39.554° was observed for HBPEN-supported PdNPs. LPEN-supported PdNPs showed the largest diffraction angle in comparison with HBPEN- and HBPEN copolymer-supported PdNPs. The difference in diffraction angle reflects the size of PdNPs; PdNPs supported by LPEN were clearly larger than PdNPs supported by HBPEN or HBPEN copolymer.

CONCLUSION

A novel HBPEN and its copolymer were synthesized as supports for PdNPs. Soluble HBPEN and its copolymer were obtained by self-polycondensation of the AB_2 monomer with or without AB monomer. A study of the model reaction suggests the formation of HBPEN with a DB of 0.37. The coordination of nitrile groups in the repeating unit with Pd^{2+} was confirmed by IR measurements. The reduction of the coordinated complexes with $NaBH_4$ results in the formation of HBPEN-, HBPEN copolymer- and LPEN-supported PdNPs. Both TEM images and X-ray diffraction patterns suggest that PdNPs supported by HBPEN were the smallest in size among these three polymers. A comparison of the three PdNPs suggests that the branched architecture in HBPEN can help prevent the aggregation of PdNPs generated in the early stage of the reduction. In general, hyperbranched polymers have potential advantages over dendrimers because of their ease of production. This study implies that the coordination of metal ions in the irregular dendritic architecture of hyperbranched polymers contributes to the formation of small metal NPs, similar to dendrimers.

CONFLICT OF INTEREST

The authors declare no conflict of interest.

ACKNOWLEDGEMENTS

We acknowledge Mr Takahiro Yamaya for XPS measurements and elemental analyses.

1 Shipway, A. N., Katz, E. & Willner, I. Nanoparticle arrays on surfaces for electronic, optical, and sensor applications. *Chem. Phys. Chem.* **1**, 18–52 (2000).
2 Sharma, V. K., Yngard, R. A. & Lin, Y. Silver nanoparticles: green synthesis and their antimicrobial activities. *Adv. Colloid Interface Sci.* **145**, 83–96 (2009).
3 Daniel, M. C. & Astruc, D. Gold nanoparticles: assembly, supramolecular chemistry, quantum-size-related properties, and applications toward biology, catalysis, and nanotechnology. *Chem. Rev.* **104**, 293–346 (2004).
4 Deraedt, C. & Astruc, D. 'Homeopathic' palladium nanoparticle catalysis of cross carbon-carbon coupling reactions. *Acc. Chem. Res.* **47**, 494–503 (2014).
5 Haruta, M. & Daté, M. Advances in the catalysis of Au nanoparticles. *Appl. Cat. A* **222**, 427–437 (2001).
6 Brust, M., Walker, M., Bethell, D., Schiffrin, D. J. & Whyman, R. Synthesis of thiol-derivatised gold nanoparticles in a two-phase liquid-liquid system. *J. Chem. Soc. Chem. Commun.* 801–802 (1994).
7 Hirai, H., Wakabayashi, H. & Komiyama, M. Preparation of polymer-protected colloidal dispersions of copper. *Bull. Chem. Soc. Jpn.* **59**, 367–372 (1986).
8 Haruta, M. Size- and support-dependency in the catalysis of gold. *Catal. Today* **36**, 153–166 (1997).
9 Teranishi, T. & Miyake, M. Size control of palladium nanoparticles and their crystal structures. *Chem. Mater.* **10**, 594–600 (1998).
10 Teranishi, T., Hosoe, M., Tanaka, T. & Miyake, M. Size control of monodispersed Pt nanoparticles and their 2D organization by electrophoretic deposition. *J. Phys. Chem. B* **103**, 3818–3827 (1999).
11 Crooks, R. M., Zhao, M., Sun, L., Chechik, V. & Yeung, L. K. Dendrimer-encapsulated metal nanoparticles: Synthesis, characterization, and applications to catalysis. *Acc. Chem. Res.* **34**, 181–190 (2001).
12 Yamamoto, K. & Imaoka, T. Precision synthesis of subnanoparticles using dendrimers as a superatom synthesizer. *Acc. Chem. Res.* **47**, 1127–1136 (2014).
13 Ye, H. & Crooks, R. M. Effect of elemental composition of PtPd bimetallic nanoparticles containing an average of 180 atoms on the kinetics of the electrochemical oxygen reduction reaction. *J. Am. Chem. Soc.* **129**, 3627–3633 (2007).
14 Ye, H. & Crooks, R. M. Electrocatalytic O_2 reduction at glassy carbon electrodes modified with dendrimer-encapsulated Pt nanoparticles. *J. Am. Chem. Soc.* **127**, 4930–4934 (2005).
15 Ye, H., Crooks, J. A. & Crooks, R. M. Effect of particle size on the kinetics of the electrocatalytic oxygen reduction reaction catalyzed by Pt dendrimer-encapsulated nanoparticles. *Langmuir* **23**, 11901–11906 (2007).
16 Scott, R. W. J., Wilson, O. M., Oh, S.-K., Kenik, E. A. & Crooks, R. M. Bimetallic palladium-gold dendrimer-encapsulated catalysts. *J. Am. Chem. Soc.* **126**, 15583–15591 (2004).
17 Scott, R. W. J., Datye, A. K. & Crooks, R. M. Bimetallic palladium–platinum dendrimer-encapsulated catalysts. *J. Am. Chem. Soc.* **125**, 3708–3709 (2003).
18 Oh, S.-K., Niu, Y. & Crooks, R. M. Size-selective catalytic activity of Pd nanoparticles encapsulated within end-group functionalized dendrimers. *Langmuir* **21**, 10209–10213 (2005).
19 Ogasawara, S. & Kato, S. Palladium nanoparticles captured in microporous polymers: a tailor-made catalyst for heterogeneous carbon cross-coupling reactions. *J. Am. Chem. Soc.* **132**, 4608–4613 (2010).
20 Huang, W., Kuhn, J. N., Tsung, C.-K., Zhang, Y., Habas, S. E., Yang, P. & Somorjai, G. A. Dendrimer templated synthesis of one nanometer Rh and Pt particles supported on

mesoporous silica: catalytic activity for ethylene and pyrrole hydrogenation. *Nano Lett.* **8**, 2027–2034 (2008).
21 Garcia-Martinez, J. C., Lezutekong, R. & Crooks, R. M. Dendrimer-encapsulated Pd nanoparticles as aqueous, room-temperature catalysts for the Stille reaction. *J. Am. Chem. Soc.* **127**, 5097–5103 (2005).
22 Garcia-Martinez, J. C. & Crooks, R. M. Extraction of Au nanoparticles having narrow size distributions from within dendrimer templates. *J. Am. Chem. Soc.* **126**, 16170–16178 (2004).
23 Imaoka, T., Kitazawa, H., Chun, W. J., Omura, S., Albrecht, K. & Yamamoto, K. Magic number Pt13 and misshapen Pt12 clusters: which one is the better catalyst? *J. Am. Chem. Soc.* **135**, 13089–13095 (2013).
24 Wilms, D., Stiriba, S.-E. & Frey, H. Hyperbranched polyglycerols: from the controlled synthesis of biocompatible polyether polyols to multipurpose applications. *Acc. Chem. Res.* **43**, 129–141 (2010).
25 Liu, J., Huang, W., Pang, Y. & Yan, D. Hyperbranched polyphosphates: synthesis, functionalization and biomedical applications. *Chem. Soc. Rev.* **44**, 3942–3953 (2015).
26 Voit, B. I. & Lederer, A. Hyperbranched and highly branched polymer architectures—synthetic strategies and major characterization aspects. *Chem. Rev.* **109**, 5924–5973 (2009).
27 Jikei, M. & Kakimoto, M. Hyperbranched polymers: a promising new class of materials. *Prog. Polym. Sci.* **26**, 1233–1285 (2001).
28 Sunder, A., Krämer, M., Hanselmann, R., Mülhaupt, R. & Frey, H. Molecular nanocapsules based on amphiphilic hyperbranched polyglycerols. *Angew. Chem. Int. Ed.* **38**, 3552–3555 (1999).
29 Shlotterbeck, U., Aymonier, C., Thomann, R., Hofmeister, H., Tromp, M., Richtering, W. & Mecking, S. Shape-selective synthesis of palladium nanoparticle stabilized by highly branched amphiphilic polymers. *Adv. Func. Mater* **14**, 999–1004 (2004).
30 Sablong, R., Schlotterbeck, U., Vogt, D. & Mecking, S. Catalysis with soluble hybrids of highly branched macromolecules with palladium nanoparticles in a continuously operated membrane reactor. *Adv. Synth. Catal.* **345**, 333–336 (2003).
31 Mecking, S., Thomann, R., Frey, H. & Sunder, A. Preparation of catalytically active palladium nanoclusters in compartments of amphiphilic hyperbranched polyglycerols. *Macromolecules* **33**, 3958–3960 (2000).
32 Chen, Y., Frey, H., Thomann, R. & Stiriba, S.-E. Optically active amphiphilic hyperbranched polyglycerols as templates for palladium nanoparticles. *Inorg. Chim. Acta* **359**, 1837–1844 (2006).
33 Zhang, Y., Peng, H., Huang, W., Zhou, Y., Zhang, X. & Yan, D. Hyperbranched poly (amidoamine) as the stabilizer and reductant to prepare colloid silver nanoparticles *in situ* and their antibacterial activity. *J. Phys. Chem. C* **112**, 2330–2336 (2008).
34 Tabuani, D., Monticelli, O., Komber, H. & Russo, S. Preparation and characterisation of Pd nanoclusters in hyperbranched aramid templates to be used in homogeneous catalysis. *Macromol. Chem. Phys.* **204**, 1576–1583 (2003).
35 Tabuani, D., Monticelli, O., Chincarini, A., Bianchini, C., Vizza, F., Moneti, S. & Russo, S. Palladium nanoparticles supported on hyperbranched aramids: synthesis, characterization, and some application in the hydrogenation of unsaturated substrates. *Macromolecules* **36**, 4294–4301 (2003).
36 Sun, X., Dong, S. & Wang, E. One-step preparation and characterization of poly (propyleneimine) dendrimer-protected silver nanoclusters. *Macromolecules* **37**, 7105–7108 (2004).
37 Skaria, S., Thomann, R., Gómez-Garcia, C. J., Vanmaele, L., Loccufier, J., Frey, H. & Stiriba, S.-E. A convenient approach to amphiphilic hyperbranched polymers with thioether shell for the preparation and stabilization of coinage metal (Cu, Ag, Au) nanoparticles. *J. Polym. Sci. Part A* **52**, 1369–1375 (2014).
38 Péringnon, N., Mingotaud, A.-F., Marty, J.-D., Rico-Lattes, I. & Mingotaud, C. Formation and stabilization in water of metal nanoparticles by a hyperbranched polymer chemically analogous to PAMAM dendrimers. *Chem. Mater.* **16**, 4856–4858 (2004).
39 Pérignon, N., Marty, J.-D., Mingotaud, A.-F., Dumont, M., Rico-Lattes, I. & Mingotaud, C. Hyperbranched polymers analogous to PAMAN dendrimers for the formation and stabilization of gold nanoparticles. *Macromolecules* **40**, 3034–3041 (2007).
40 Marty, J. D., Martinez-Aripe, E., Mingotaud, A. F. & Mingotaud, C. Hyperbranched polyamidoamine as stabilizer for catalytically active nanoparticles in water. *J. Colloid Interface Sci.* **326**, 51–54 (2008).
41 Krämer, M., Pérignon, N., Haag, R., Marty, J.-D., Thomann, R., Viguerie, N. L. & Mingotaud, C. Water-soluble dendritic architectures with carbohydrate shells for the templation and stabilization of catalytically active metal nanoparticles. *Macromolecules* **38**, 8308–8315 (2005).
42 Jikei, M., Itoh, H., Yoshida, N., Inai, Y., Hayakawa, T. & Kakimoto, M.-A. Synthesis of hyperbranched poly(ether nitrile)s by one-step polycondensation of an AB_2 monomer. *J. Polym. Sci. Part A* **47**, 5835–5844 (2009).
43 He, Q., Xu, T., Qian, H., Zheng, J., Shi, C., Li, Y. & Zhang, S. Enhanced proton conductivity of sulfonated poly(p-phenylene-co-aryl ether ketone) proton exchange membranes with controlled microblock structure. *J. Power Sources* **278**, 590–598 (2015).
44 Lee, M., Yoo, Y.-S. & Choi, M.-G. Synthesis and mesomorphic properties of palladium (II) complexes based on 3,4,5-trialkoxy benzonitrile ligands. *Bull. Korean Chem. Soc.* **18**, 1067–1070 (1997).
45 Martínez, C. A. & Hay, A. S. Synthesis of poly(aryl ether) dendrimers using an aryl carbonate and mixtures of metal carbonates and metal hydroxides. *J. Polym. Sci. Part A* **35**, 1781–1798 (1997).
46 Hölter, D. & Frey, H. Degree of branching in hyperbranched polymers. 2. Enhancement of the DB: Scope and limitations. *Acta Polym.* **48**, 298–309 (1997).
47 Matsuo, S., Murakami, T. & Takasawa, R. Synthesis and properties of new crystalline poly(arylene ether nitriles). *J. Polym. Sci. Part A* **31**, 3439–3446 (1993).
48 Yamauchi, M. & Kitagawa, H. Hydrogen absorption of the polymer-coated Pd nanoparticle. *Synth. Met.* **153**, 353–356 (2005).
49 Ohba, T., Kubo, H., Ohshima, Y., Makita, Y., Nakamura, N., Uehara, H., Takakusagi, S. & Asakura, K. EXAFS studies of Pd nanoparticles: direct evidence for unusual Pd–Pd bond elongation. *Chem. Lett.* **44**, 803–805 (2015).

Supplementary Information accompanies the paper on Polymer Journal website (http://www.nature.com/pj)